

## CHAPTER 1

# **Introduction and Overview**

## 1.1 Introduction

The first interstellar molecules to be discovered were CH, CN and CH<sup>+</sup>. UV lines of these molecules were observed in absorption (Spitzer 1968). Considering that the range of optical observations is limited due to extinction, and due to the advent of radio astronomy, Shklovski (1952) and Townes (1957) produced a list of molecules that may be detectable at radio frequencies. The first of these detections was that of the hydroxyl radical, observed in absorption against Cas A, by Weinreb et al. (1963). The discovery of Carbon Monoxide, by Wilson et al. (1971) was the first observation of a millimeter wave transition. It has led to many new discoveries concerning interstellar and circumstellar matter, and the structure and kinematics of the Milky Way and many other galaxies. In circumstellar envelopes, CO was first detected by Solomon et al. (1971).

Most of the transitions observed from interstellar and circumstellar molecules are rotational transitions where the excitation to the upper level is mainly by collisions with hydrogen molecules and in most circumstances the excitation temperature deduced from the populations of the concerned levels equals the kinetic temperature. A departure from this situation has been observed in two cases: 1. Anomalous absorption by H<sub>2</sub>CO where the excitation temperature implied by observations is less than 1.7K, i.e., the molecule is seen in absorption against the 2.7K cosmic background radiation (Palmer et al. 1969). 2. The other situation is that of population inversion in OH masers which was first noticed as intense emission at 1612 MHz by Wilson and Barrett (1968).

Astronomical maser emission is found in a wide variety of objects such as, comets (OH maser, Biraud et al. 1974), planets (CO<sub>2</sub> 10 micron maser, Mumma et al. 1983), stars, molecular clouds and galactic nuclei. Such emission has been

observed in rotational transitions for eight molecular species so far: OH, H<sub>2</sub>O, SiO, HCN, CH<sub>3</sub>OH, H<sub>2</sub>CO, CO<sub>2</sub> and SiS. In Table 1 we list some properties of these masers and the environment in which they occur.

Rotational transitions from thermally populated levels have been observed from several molecular species. Although this emission is easier to interpret than the maser emission, it arises from a relatively larger volume of gas than that of the maser emission. By understanding how the maser works, one can use it as a probe to study the processes occurring over very small (milli-arcsecond) angular scales in e.g., star-forming regions or circumstellar shells of late-type stars. Apart from acting as probes, astronomical masers remain interesting natural phenomena in themselves, with many questions as yet completely unresolved.

Maser emission from silicon monoxide was first observed by Snyder and Buhl in 1974, from the Orion molecular cloud. OH maser emission was by then well known to be associated with late-type stars (Wilson and Barrett 1972, Knowles et al. 1969, Schwartz and Barrett 1970, Robinson et al. 1971, Rieu et al. 1971). Since the line-profile observed by Snyder and Buhl was double-peaked like a typical OH spectrum from a Mira variable, Kaifu, Snyder and Buhl (1975) assumed that the centroid velocity of the spectrum from Orion corresponded to the velocity of the molecular cloud, and used this fact to identify this emission as the  $v=1$   $J = 2 \rightarrow 1$  transition of SiO. They also detected this line in several Mira variables. Several searches for this emission from HII regions similar to Orion, were made but none led to any detection (Spencer et al. 1977, Genzel et al. 1980) and Orion remained a unique object showing the SiO maser emission among star forming regions (Elitzur 1982, Ukita and Goldsmith 1984, Barvainis and Clemens 1984). More recently however, SiO masers have been detected in

Table 1: Astronomical Masers

Masing molecule	Site <sup>a</sup>	Frequency	$T_B$ (K)	Density <sup>b</sup>
OH	Comets	1665 MHz		$3.3 \times 10^{12} \text{cm}^{-2}$
	Stars	1612, 1665 MHz	$10^8$	$10^4 \text{cm}^{-3}$
	Mol. Clouds	1665 MHz	$10^{12}$	
H <sub>2</sub> O	Galactic Nuclei	1612 MHz	$5 \times 10^2 - 3 \times 10^6$	$3.6 \times 10^{17} \text{cm}^{-2}$
	Stars	22 GHz	$10^{11}$	$10^9 \text{cm}^{-3}$
	Mol. Clouds	22 GHz	$10^{14}$	
SiO	Galactic Nuclei	22 GHz		
	Stars	43, 86 GHz	$10^{10}$	$10^{10} \text{cm}^{-3}$
CH <sub>3</sub> OH	Mol. Clouds	86 GHz		$10^5 \text{cm}^{-3}$
	Mol. Clouds	12, 25 GHz		$2 \times 10^6 \text{cm}^{-3}$
H <sub>2</sub> CO	Mol. Clouds	4.8 GHz		$3 \times 10^4 \text{cm}^{-3}$
CO <sub>2</sub>	Planets	$3 \times 10^{13}$ Hz	$10^8$	$2 \times 10^{14} \text{cm}^{-2}$
HCN	Stars			
SiS	Stars			
Masing molecule	Site <sup>1</sup>	$T_k$	Size (gain-length)	Filling factor <sup>c</sup>
OH	Comets		$10^6 \text{km}$	
	Stars	30		$10^3/1$
	Mol. Clouds			$10/1$
H <sub>2</sub> O	Galactic Nuclei	40	350 pc	
	Stars	1000	$10^{14} \text{cm}$	$10/0.1$
	Mol. Clouds		$10^{14} - 10^{16}$	$1/1$
SiO	Galactic Nuclei			
	Stars	2000		$10/0.1$
CH <sub>3</sub> OH	Mol. Clouds			
	Mol. Clouds	90		$< 2/2$
H <sub>2</sub> CO	Mol. Clouds	40		
CO <sub>2</sub>	Planets	150	$10^5 - 10^6$	
HCN	Stars			
SiS	Stars	200		

<sup>a</sup>Circumstellar.<sup>b</sup>Column densities refer to the masing molecules and Volume densities refer to the density of gas.<sup>c</sup>Ratio of size of masing spots to the angle subtended by their distribution, milli-arcseconds/arcseconds.

two other molecular clouds W51 and Sgr B2-MD5 (Ukita et al. 1985). Several new detections from Mira variables were made in the SiO  $J = 2 \rightarrow 1$  and  $J = 1 \rightarrow 0$  transitions in the  $v=1$  state, and it began to appear that most Mira variables might be emitting the SiO maser lines (Snyder and Buhl 1975, Blair and Dickinson 1977, Spencer et al. 1977, Dickinson et al. 1978, Lepine et al. 1978, Engels et al. 1979). Detections were also reported from higher rotational transitions. There were some indications regarding the types of Mira variables that may be maser sources (Cahn 1977, Spencer et al. 1977) but these were tentative and not confirmed. So far, about 190 late-type stars have been observed by millimeter wave telescopes, and about 40% of them have shown the maser emission. (Engels and Heske 1989). Most of these observations have been restricted to late spectral types. In this thesis, we present observations of about 180 Mira variables spread in spectral-types from h13 to M10. We establish that the maser emission is restricted to those sources which are later than M6 in spectral type, with the exception of super-giants. Since this thesis concentrates on the SiO maser and its relationship to the nature of Mira variables, in the following two sections we give some properties of the SiO molecule and briefly also of the Mira variables and their atmospheres. Finally, we list in detail, the characteristics of the SiO maser as inferred from all the observations available so far.

## 1.2 SiO molecular parameters

The molecular constants and rotational spectrum of silicon monoxide have been measured experimentally by Manson et al. (1977). These measurements provide accurate rest frequencies for all the astronomically observed SiO transitions as well as molecular parameters which can be used to calculate the frequencies of other transitions, including those of the isotopes of SiO. Fig. 1 shows the energy levels of SiO, indicating the transitions observed so far, from astronomical objects. Our observations were only those of the  $J = 2 \rightarrow 1$  transition in the  $v=1$  state at 86 GHz. In Table 2, we list the values of frequencies of various transitions for reference, and the Einstein A coefficients for spontaneous emission in rotational transitions which are calculated according to the following formulae (Herzberg 1950). The energy of a vibrating rotor, is given by,

$$E = \omega_e(v + 1/2) - \omega_e x_e(v + 1/2)^2 + \dots + B_v J(J + 1) - D_v J^2(J + 1)^2 + \dots,$$

where  $B_v = B_e - \alpha_e(v + 1/2)$  and  $D_v = D_e + \beta_e(v + 1/2)$ , and  $\alpha_e$  and  $\beta_e$  are small constants. The A coefficient for a rotational transition is given by,

$$A_{J+1 \rightarrow J} = \frac{64\pi^4}{3hc^3} \nu^3 \frac{J+1}{2J+1} \mu^2,$$

where  $\mu$  is the dipole moment of SiO,  $3.098 \times 10^{-18}$  esu cm. The A coefficient for the vibrational-rotational transition can be calculated from,

$$A_{vJ \rightarrow v'J'} = A_{vv'} \frac{S_{JJ'}}{g_J},$$

where,  $S_{JJ'} = J' + 1$  for R branch and  $S_{JJ'} = J'$  for P branch.

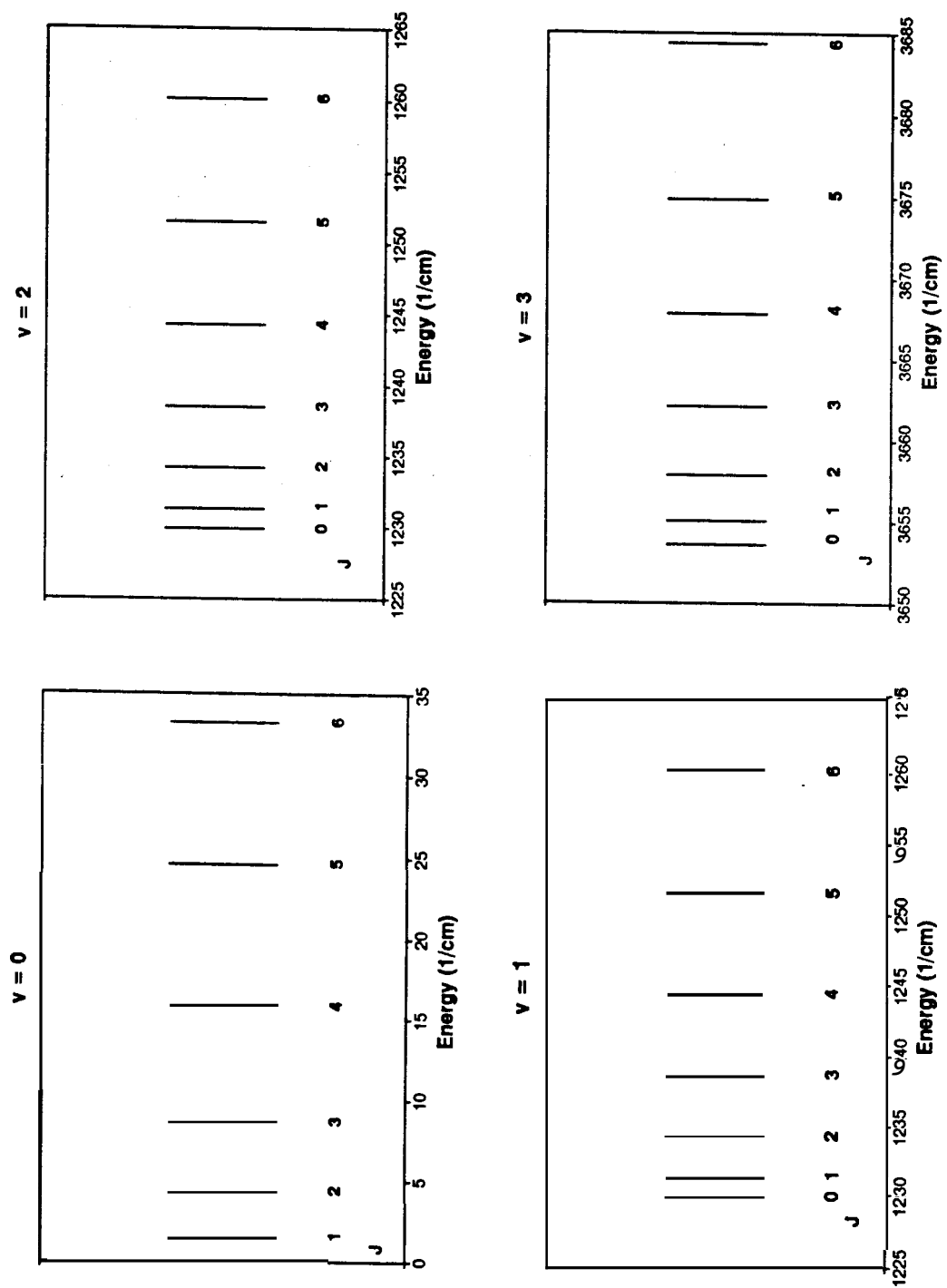


Figure 1: Energy-levels of SiO molecule

Table 2: SiO molecular parameters

Equilibrium internuclear distance	$r_e$	1.5097 Å
Rotational constant	$B_e$	21787.5 MHz
Harmonic vibrational frequency constant	$w_e$	1252.3 $\text{cm}^{-1}$
Anharmonic vibrational frequency constant	$w_e x_e$	5.96 $\text{cm}^{-1}$
Dissociation energy	$D_o$	7.93 $\pm$ 0.13 eV

$v$	J (upper)	Frequency (MHz)	$A$ ( $s^{-1}$ ) (rotational transitions)
0	1	43423.76	$9.1296 \times 10^{-6}$
	2	86846.96	$4.8690 \times 10^{-5}$
	3	130268.61	$1.4789 \times 10^{-4}$
	4	173688.31	$3.3385 \times 10^{-4}$
	5	217104.98	$6.3388 \times 10^{-4}$
	6	260518.02	$1.0753 \times 10^{-3}$
1	1	43122.03	$8.9406 \times 10^{-6}$
	2	86243.37	$4.7682 \times 10^{-5}$
	3	129363.24	$1.4483 \times 10^{-4}$
	4	172481.15	$3.2693 \times 10^{-4}$
	5	215595.95	$6.2076 \times 10^{-4}$
	6	258707.45	$1.0531 \times 10^{-3}$
2	1	42820.48	$8.7544 \times 10^{-6}$
	2	85640.46	$4.6689 \times 10^{-5}$
	3	128458.80 *	$1.4181 \times 10^{-4}$
	4	171275.28	$3.2012 \times 10^{-4}$
	5	214088.54	$6.0783 \times 10^{-4}$
	6	256898.56 *	$1.0311 \times 10^{-3}$
3	1	42519.34	$8.5710 \times 10^{-6}$
	2	85037.96 *	$4.5711 \times 10^{-5}$
	3	127555.18 *	$1.3884 \times 10^{-4}$
	4	170070.35	$3.1341 \times 10^{-4}$
	5	212582.60	$5.9509 \times 10^{-4}$
	6	255091.32 *	$1.0095 \times 10^{-3}$

\* Theoretical values



The values of  $A_{v',v''}$ , for the vibrational transition  $v' \rightarrow v''$  are roughly as follows (Hedelund and Lambert 1979),

Transition	$A (s^{-1})$
1 $\rightarrow$ 0	5
2 $\rightarrow$ 1	10
3 $\rightarrow$ 2	15
4 $\rightarrow$ 3	20

The values corresponding to  $A_v > 1$  are less than one.

### 1.3 Mira variables: a brief description

A typical Mira variable has the following physical description:

**Table 3: Mira variables — Typical properties**

Luminosity	$\approx 10^4 L_\odot$
Mass	$\approx 1.2 M_\odot$
Effective Temperature	1800-3500 K
Radius	$\approx 250 R_\odot$
Pulsational period	350 days
Visual Amplitude	6 magnitudes

The values of period and amplitude represent the mean of the distribution which extends from 100 to 1000 days in period and 2.5 to 10 magnitudes in visual amplitude. The histograms of the number of Mira variables in our galaxy, as a function of period, amplitude and spectral types can be found in Kukarkin (1973). The term “Mira” is characterized by the variability of the light. It does not specify the spectral type of the star. For example, all the stars in the following table are called Mira variables though they have different spectral types and therefore different effective temperatures, ages or chemical compositions.

M type:	R Leo, R Aql, o Cet, R Cae, R Cen, R Hya...
S type:	R And, R Cyg, $\chi$ Cyg,...
C type:	U Cyg, V Cyg, T Dra, R Lep, SS Vir...

The class M represents stars showing deep absorption bands due to oxides of metals like titanium and vanadium. The class S stars exhibit Zr, Y and Ba oxides. The class C represents carbon stars showing spectral features from CN, CH and C<sub>2</sub> etc. The class M forms the largest group of the three. The variability of these stars is classified as M, SRa, SRb, SRc and IR, in decreasing order of regularity in the variation. The semi-regular types (SRa...) have lower pulsational amplitudes and larger periods. The supergiant stars VX Sgr and S Per for example, fall in this class. The spectral differences between the stars of various degrees of regularity but a single spectral class are not considerable. Now to which spectral types do Mira variables showing SiO maser emission belong? It is known that only Mira variables of the spectral type M show the masers but with the following known exceptional cases: W And and  $\chi$  Cyg are the only two S type Miras showing maser emission and T Cep, a well known SiO maser source, is a borderline case between M and S types (Blair and Dickinson 1977). The C type stars show a greater abundance of carbon relative to oxygen; thus, in these stars one expects that Si will combine more often with carbon than with oxygen. In Chapter 4, we report a tentative detection of SiO maser emission from one such star, T Cnc.

The atmospheres of these stars are very extended and present a site for many interesting physical processes. The pulsations can induce shock waves in the lower part of the atmosphere, initiating the process of mass loss. Numerical studies of the dynamics of atmospheres also support this (Bowen 1988 and references therein). It is interesting to note that the locations of SiO masers seem to be in this part of the atmosphere, i.e., within 3 to 5 stellar radii. This is inferred from VLBI maps and from the fact that the emission arises from excited

vibrational states whose energies correspond to at least 1800 K. At this location, the dynamics of the atmosphere is very complicated by the presence of shocks, and both outflow as well as infall of matter. How the maser emission is affected by this dynamics is not yet clear. From the time variation of maser line profiles there have been some indications of the influence of the shocks on the masers (Troland et al. 1979, Clark et al. 1982). We attempt to give an overview of this aspect of the maser problem, in Chapter 7. The gaseous envelope itself exhibits rich chemistry and more than 60 molecular species are seen so far at millimeter wavelengths. Several sensitive observations have been made of these rotational lines and one finds that the line profiles agree with the calculated ones. The model calculations make use of the fact that the level populations get affected by radiation that arises only from a small neighbourhood whose extent depends on the velocity gradient and the temperature of the region. This fact simplifies the radiative transfer (Castor 1970). The excitation of levels is assumed to be primarily due to collisions with hydrogen molecules. The line-widths and the number densities give an estimate of the mass-loss rate. For example from CO observations, the deduced mass loss rate is of the order of  $10^{-6}$  to  $10^{-5}$  solar masses per year.

Broad-band spectrometry in the range of 3 to 14  $\mu$  revealed an excess over the blackbody emission (Woolf and Ney 1969). This was interpreted as emission coming from the circumstellar rather than the chromospheric region. This interpretation is simpler because the molecules known to exist in the chromosphere do not seem to have strong emission bands in this spectral region and any new species should also have shown up at other frequencies. Therefore, it was suspected that this emission is from circumstellar solid particles. Moreover,

this emission is unlike to that from a black-body of a different temperature and angular extent, but it is sharply peaked, which indicates a similar wavelength dependence of the opacity of the material. From a comparison of this broad band spectrum with a laboratory spectrum, the constituents were seen to be  $\text{MgSiO}_3$  (about 80%),  $\text{SiO}_2$ ,  $\text{Fe}_2\text{O}_3$  and  $(\text{Mg, Fe})_2\text{SiO}_4$  (Gaustad 1963). Earlier, Hoyle and Wickramasinghe (1962), had suggested that the interstellar extinction of 1 mag per kpc at 4000 angstroms may be due to graphites and not due to ice and that these particles may be produced in the cooler envelopes of red-giants and ejected out into the interstellar medium by radiation pressure. This was worked out in detail by Salpeter (1977). Thus we see that complex molecules form in the outer part of the envelope which is cooler (800K).

Later in Chapter 7 we shall discuss the circumstellar dust emission and its relation to the maser phenomenon.

The evolutionary status of the Mira variables on a schematic H-R diagram is shown in Fig. 2. These stars have degenerate carbon or oxygen cores surrounded by thin shells of helium and hydrogen. These shells burn alternately, causing thermal pulses which lift the heavier elements from the core towards the surface of the star. It is in this epoch that the star is unstable and starts pulsating. The pulsations are sustained by a mechanism that is believed to be similar to the one operating in cepheid variables, i.e., opacity that depends on the temperature and density, such that when the gas expands, the opacity decreases and the matter tends to fall in, leading to contraction of the gas which now increases the opacity and absorbs the radiation and expands again. This opacity is contributed by  $\text{H}_e^+$  in the cepheids. In Mira variables an additional source is believed to be  $\text{He}^{++}$ . The presence of convection however, makes it difficult for this mechanism to explain

the sustenance of pulsation, and this question is not settled yet. As these stars pulsate, they perform a loop in the H-R diagram (Keeley 1970) due to the fact that their light-curves and temperature variations are asymmetrical. While the SiO maser's time variation has been studied with respect to the variation of the visual magnitude of the star, it has not yet been compared with the variation in the effective temperature. This relationship is explored in Chapter 5. In concluding this paragraph, we show a schematic diagram describing the structure of a typical circumstellar envelope in Fig. 3. The location of various masers is also shown.

## **1.4 Observational characteristics of SiO maser emission**

### **1.4.1 Relation between emission from different transitions**

As seen from Fig. 1, most of the masing transitions are in the excited vibrational states. The emission from rotational transitions in the  $v=0$  state is generally found to be weak, broad and parabolic in shape, as expected from thermal emission. Exceptions to this have been observed in Orion by Genzel et al. (1980), in VY CMa by Buhl et al. (1975) and in four more sources observed by Jewell et al. (1985), where this emission in the ground vibrational state appears to be strong and narrow and is possibly maser emission. The emission from  $J = 1 \rightarrow 0$  generally shows more number of narrow features within the profile, compared to that in  $J = 2 \rightarrow 1$  (Snyder and Buhl 1975). The photon luminosities in the  $J = 1 \rightarrow 0$  upto  $J = 5 \rightarrow 4$  transitions are probably comparable (Clemens and Lane 1983), as discussed in section 7.4; and current models fail to explain

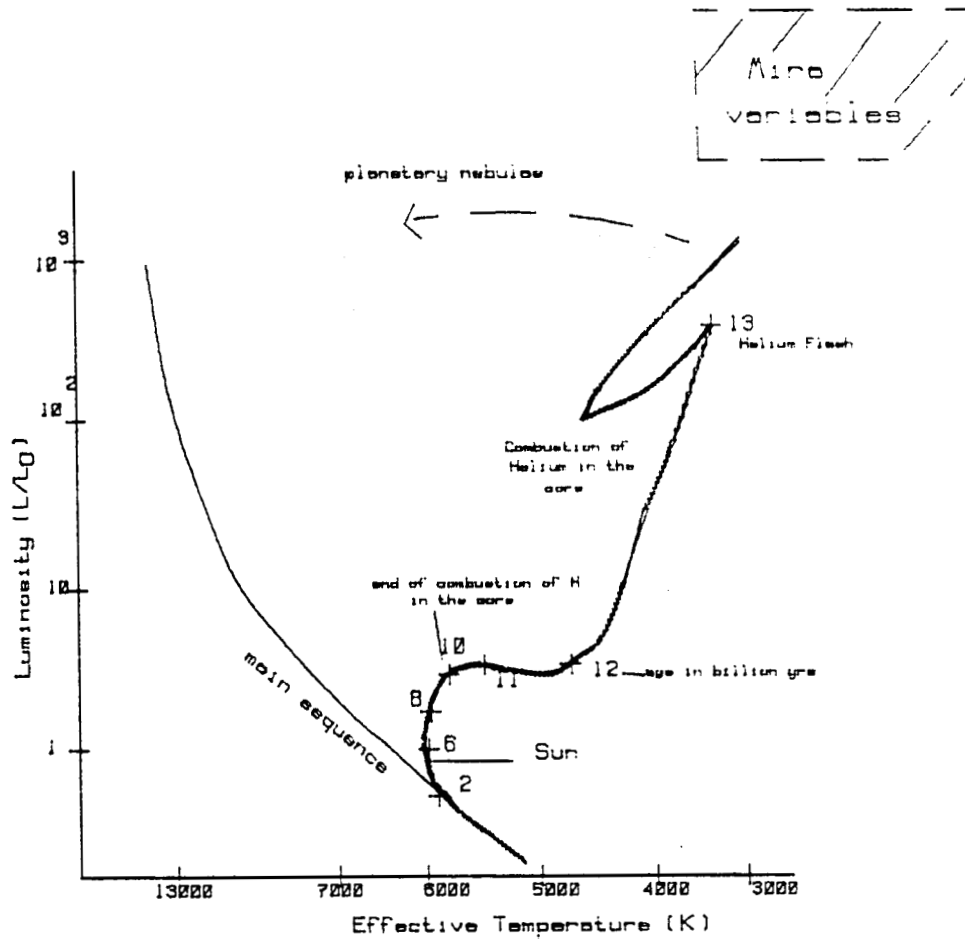


Figure 2: Schematic H-R diagram showing the location of Mira variables. The dashed-line box indicates approximately, the region of stars in our sample.

\* Adapted from The *Cambridge Atlas of Astronomy* 1985, Ed: J. Audouze & G. Israel, Cambridge Univ. Press, p 254.

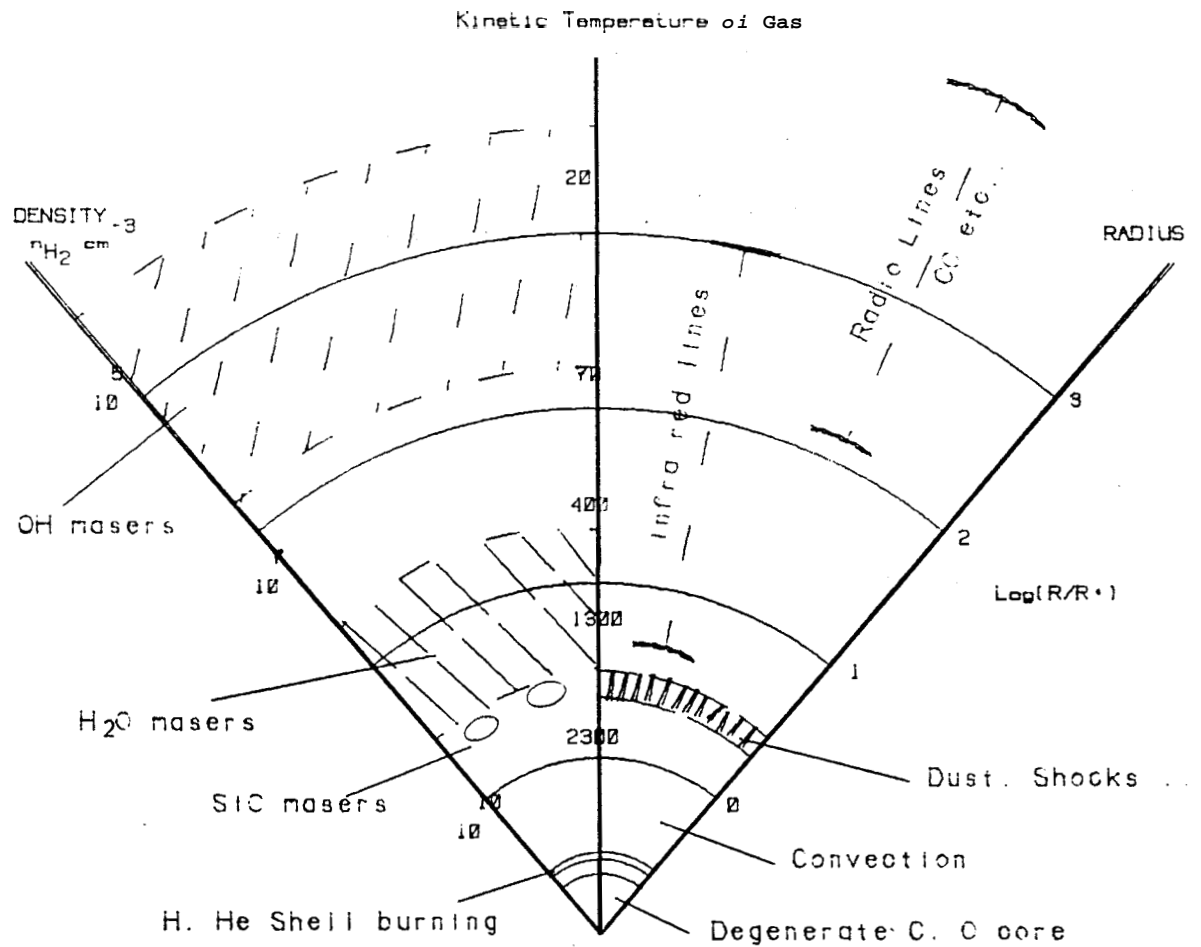


Figure 3: Schematic diagram describing the atmosphere of a Mira variable. Adapted from Omont (1985).

this fact. Comparison of polarization in different transitions indicate that same  $J$  but different  $v$  arise from the same volume of gas but same  $v$  and different  $J$  lines arise from different regions (Barvainis and Predmore 1985). However, in  $\chi$  Cyg, Olofsson et al. (1985) find that the  $v=2$  emission is sharply peaked and distinctly phase lagged with respect to the  $v=1$  emission. They also have different velocity structures, suggesting different emitting regions. Simultaneous observations in  $v=1,2$  and 3 using the same spectrometer, reported by B. Allen (1984, MIT thesis) show that interestingly there is a relative redshift between the different  $v$  states, and that it increases with  $v$ .

### **1.4.2 Velocity structure**

In M-giant Mira variables, the emission always occurs within about 10 km/sec of the stellar velocity (In super-giants, the separation in velocities is usually larger). The stellar velocity is well represented by the centroid velocity of the thermal SiO or CO emission, which also agree with each other as seen in Fig. 4, (Reid and Dickinson 1976, Bujarrabal et al. 1986). The velocity of the SiO line is compared with the stellar velocity in Fig. 5.

### **1.4.3 Spatial distribution**

VLBI observations at 43 GHz, show that the maser emission comes from spots with angular sizes much smaller than the size of the star, and distributed over an angular extent corresponding to 3-5 stellar radii (Moran et al. 1979, Lane 1984, McIntosh et al. 1989). These spots correspond to individual velocity features in the line-profiles. The position of the Mira star with respect to this distribution of maser spots is not yet measured as it requires precision in astrometry, at



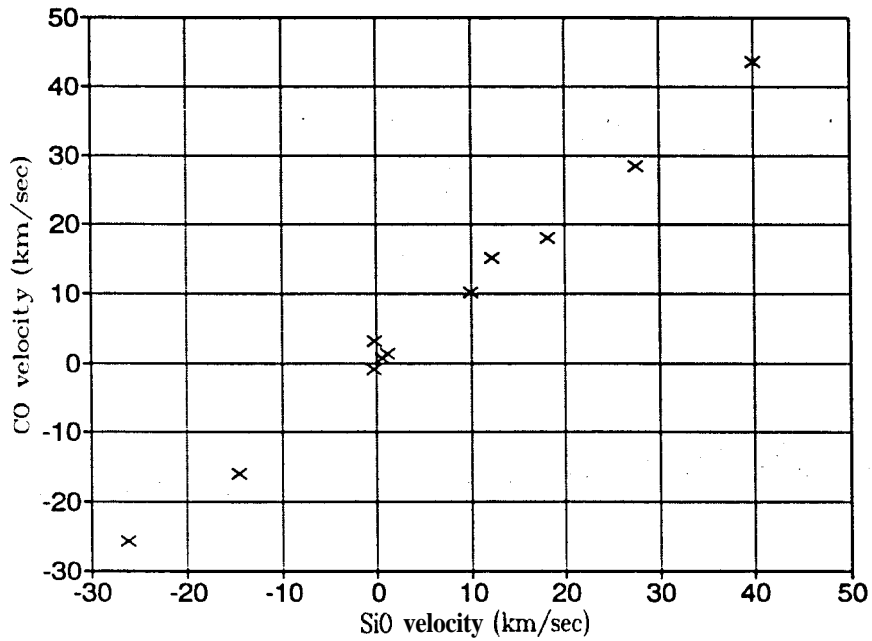


Figure 4: Plot of CO line-center velocity  $v$ /s SiO ( $v=0$ ) line-center velocity, showing the agreement between the two. This common centroid velocity represents the stellar velocity.

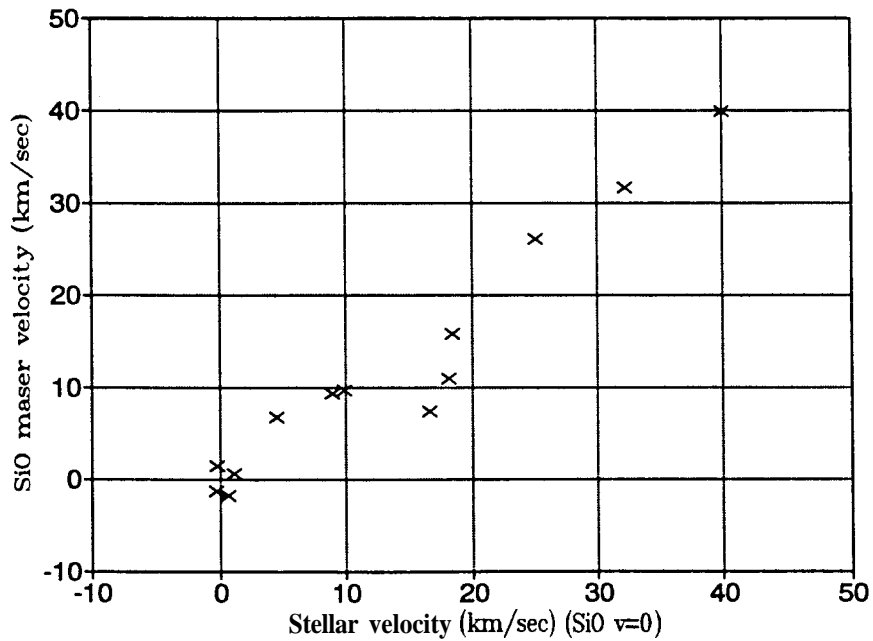


Figure 5: Plot of SiO maser velocity  $v$ /s stellar velocity, showing that the centroid velocity of the maser emission is close to the stellar velocity.

optical wavelengths, of the order of a few milli-arcseconds. Measurements of absolute positions of several well known maser sources with an rms of 0.15" in the co-ordinates, have been recently reported by Wright et al. (1990). Time variation of the spatial locations of the maser spots was seen for the first time, on comparing the recent observations of McIntosh et al. (1989) with those of Lane et al. (1984); but more such observations are needed to infer anything about the kinematics of the masing regions.

#### **1.4.4 Polarization**

Linear polarization seems to be a common feature in the SiO masers, (Troland et al. 1979, Clark et al. 1982). Circular polarization has also been detected from a few sources (Barvainis et al. 1987). Assuming the Zeeman effect to be the cause, magnetic field strengths of the order of 10-100 G have been estimated in the masing regions. Polarimetric VLBI observations (McIntosh et al. 1989) confirm that individual spots (which appear as velocity features in the line-profiles) have distinctly different polarization vectors. While the orientations and magnitudes of these do not appear to be random, the pattern does not lend itself to a straightforward interpretation. The strongest emission is most weakly polarized. Earlier studies (Troland et al. 1979, Clark et al. 1982) have noted variations in polarization on time-scales shorter than the periods. The velocities of individual features in the line-profile (made discernible by measuring their polarization), show changes which are smooth but not periodic. Barvainis and Predmore (1985) have made a multitransitional study of linear polarization which reveals the differences in polarization of emission from different rotational transitions in the same  $v$  state, but polarizations appear to be same for similar rotational transitions in different  $v$  states.

### **1.4.5 Time variation**

The integrated flux in the spectral lines usually show a correlation with the infra-red magnitude variation as the star pulsates. The variation in the SiO maxima and IR maxima, both lag in phase by about 0.2 with respect to the maxima in the optical light curves (Hjalmarson and Olofsson 1979 Nyman and Olofsson 1986, Martinez et al. 1988). The SiO light curves however, are hardly regular (except in the case of one source: o Cet). The SiO maxima can differ in intensity by a factor of **2–3** with respect to the maxima in different cycles. There are also cases of missing maxima noted (Martinez et al. 1988). One more interesting fact is that the weaker individual features in the profiles seem to disappear at or near the optical maximum (Clark et al. 1984, Miller et al. 1984). A novel hypothesis to explain the time-variation of SiO masers has been proposed by Curtis Struck-Marcell (1989). In this model, the source of SiO masers are Jovian like planets around the Mira variables and the source of SiO is the vaporization of the satellites of these planets by the stellar wind. In Chapter 7, we assess this model on the basis of existing time monitored observations of velocities of the maser spikes.

### **1.4.6 Relation to IR**

Bujarrabal et al. (1987) have found a good correlation between the maser flux and the 8 micron flux. They interpret this as evidence for a radiative pump, using the stellar infra-red photons. Recently, (Hall et al. 1990) have also found that the IRAS 12 micron flux is a good criterion for selecting sources for SiO detections. Referring to the IR emission from the dust shells around Mira variables, the IRAS Low Resolution Spectra have been studied by Vardya et al. (1986) and

they find a correlation between the amount of asymmetry in the light-curve, and the strength of the 10 micron feature in the Low Resolution Spectra. They also extend this correlation to SiO maser emission. Stencel et al. (1990) have drawn a connection between the chronological sequence of masers proposed by Lewis (1989), and the dust emission observed in the IRAS Low Resolution Spectra.

We have reviewed above the observational characteristics of the SiO masers. Much of the diversity in the maser phenomenon is yet to be understood theoretically. The earliest theoretical explanation for the population inversion was proposed by Kwan and Scoville (1974) soon after the discovery of SiO masers. This work, and many variations to follow, are however unable to explain the observed luminosities and many of the features mentioned above. Langer and Watson (1984) attempt a more accurate calculation but much in the observations still remains to be understood. We shall return to this aspect later in Chapter 7, while attempting to arrive at an overall consistent picture of the SiO maser phenomenon.

•

## REFERENCES

- Allen B., 1984 Ph.D. Thesis, MIT.
- Barvainis R., Predmore C. R., 1985, *Ap. J.* 288,694.
- Barvainis R., McIntosh G., Predmore C. R., 1987, *Nature* 329,613.
- Barvainis R., Clemens D. P., 1984, *Astron. J.* 89,1833.
- Biraud F., G. et al., *Astron. Astrophys.* 34,163.
- Blair G. N., Dickinson D. F., 1977, *Ap. J.* 215,552.
- Bowen G. H., 1988, *Ap. J.* 329,299.
- Buhl D., Snyder L. E., Lovas F. J., Johnson D. R., 1975, *Ap. J.* **201**,L29.
- Bujarrabal V., et al., 1986, *Astron. Astrophys.* 162,157.
- Bujarrabal V., Planesas P., Romero A., 1987, *Astron. Astrophys.* 175,164.
- Cahn J., 1977, *Ap. J. Lett.* **212**,L135.
- Castor J. I., 1970, *Mon. Not. R. Astr. Soc.* 149,111.
- Clark F. O., Troland T. H., Johnson D. R., 1982, *Ap. J.* 261,569.
- Clark F. O., Waak J. A., Bologna J. M., 1982, *Astron. J.* 87,1803.
- Clark F. O., et al., 1984, *Ap. J.* 276,572.
- Clemens D. P., Lane A. P., 1983, *Ap. J. Lett.* **266**,L117.
- Curtis Struck-Marcell, 1989, *Ap. J.* 330,986.
- Dickinson D. F., et al., 1978, *Astron. J.* **83**,36.
- Elitzur M., 1982, *Ap. J.* 262,189.
- Engels D., Heske A., 1989, *Astron. Astrophys. Suppl. Ser.* 81,323.
- Engels D., 1979, *Astron. Astrophys. Suppl. Ser.* 36,337.
- Gaustad J. E., 1963, *Ap. J.* 138,1050
- Genzel R., et al., 1980, *Ap. J.* 239,519.
- Hall P. J., et al., 1990, *Mon. Not. Royal Astron. Soc.* 243,480.
- Hedelund J., Lambert D. L., 1972, *Astrophys. Lett.* **11**,71.
- Herzberg 1950, *Molecular Spectra Vol. 1 Diatomic molecules*,  
D. Van Nostrand Co. Inc.
- Hjalmarson A., Olofsson H., 1979, *Ap. J.* **234**,L199.

- Hoyle F., Wickramasinghe N. C., 1962, *Mon. Not. Royal Astr. Soc.* 124,417.
- Jewell P. R., Walmsley C. M., Wilson T. L., Snyder L. E., 1985, *Ap. J.* **298**,L55.
- Kaifu N., Buhl D., Snyder L. E., 1975, *Ap. J.* 195,359.
- Keeley D., 1970, *Ap. J.* 161,643.
- Knowles et al. 1969, *Science* 163,1055.
- Kukarkin B. V., 1973, *Pulsating Stars*, John Wiley & Sons, p 282.
- Lane A. P., 1984, *IAU Symp 110, VLBI and compact radio sources*,  
D. Reidel Publ. Co., p 329.
- Langer S. H., Watson W. D., 1984, *Ap. J.* 284,751.
- Lepine J. R. D., LeSqueren A. M., Scalise E. Jr , 1978, *Ap. J.* 225,869.
- Lewis B. M., 1989, *Ap. J.* 338,234.
- Little-Marenin, Little S. J., 1990, *Astron. J.* 99,1173.
- Manson E. L. Jr, et al., 1977, *Phys. Rev. A* 15,223.
- Martinez A., Bujarrabal V., Alcolea J., 1988,  
*Astron. Astrophys. Supp. Ser.* **74,273**.
- McIntosh G. C., et al. 1989, *Ap. J.* 337,934.
- Miller J. S., Clark F. O., Troland T. H., 1984, *Ap. J.* **287**,892.
- Moran J. M., et al., 1979, *Ap. J.* 231,124.
- Mumma M. J., et al., 1981, *Science* 212,455.
- Nyman L. A., Olofsson H., 1986, *Astron. Astrophys.* **158**,67.
- Olofsson H., Rydbeck O. E. H., Nyman L. A., 1985, *Astron. Astrophys.* 150,169.
- Palmer P., Zuckerman B., Buhl D., Snyder L. E., 1969, *Ap. J.* **156**,L147.
- Reid M. J., Dickinson D. F., 1976, *Ap. J.* 209,505.
- Rieu N. Q., Fillit R, Gheudin M., 1971,  
*Astron. Astrophys.* 14,154.
- Robinson B. J., Caswell J. L., Goss W. M., 1971, *Astrophys. Lett.* 7,163.
- Salpeter E., 1977, *Ann. Rev. Astron. Astrophys.* 15,237.
- Schwartz P. R., Barrett A. H., 1970, *Ap. J.* **159**,L123.
- Shklovski I., 1952, *Astron. Zh.* 29,144.
- Snyder L. E., Buhl D., 1975, *Ap. J.* 197,329.
- Omont A., 1985, *Reviews in Modern Astronomy* 1, Ed.: G. Klare, p104.

- Snyder L. E., Buhl D., 1974, *Ap. J. Lett.* **189**,L31.
- Solomon P., et al., 1971 *Ap. J. Lett.* **163**,L53.
- Spencer J. H., et al., 1977, *Astron. J.* 82,706.
- Stencel R. E., Nuth J. A. III, Little-Marenin Little S. J., 1990, *Ap. J.* **350**,L45.
- Spitzer L., 1968, *Diffuse matter in space*, Interscience Publ., p 44.
- Townes C., 1957, *IAU Symp No.4*, D. Reidel Publ. Co., p 92.
- Troland T. H., Heiles C., Johnson D. R., Clark F. O., 1979, *Ap. J.* 232,143.
- Ukita N., Goldsmith P., 1984, *Astron. Astrophys.* 138,194.
- Ukita et al., 1985, *IAU symp 115 'Star-forming regions'*,  
D. Reidel Publ. Co.,p 178.
- Vardya M. S., De Jong T., Willems F. J., 1986, *Ap. J.* **304**,L29.
- Weinreb S., Barrett A. H. et al. 1963, *Nature* 200,829.
- Wilson W. J., Barrett A. H., 1972, *Astron. Astrophys.* 17,385.
- Wilson R. W., Jefferts K. B., Penzias A. A., 1971, *Ap. J.* **161**,L43.
- Woolf N. J., Ney E. P., 1969, *Ap. J. Lett.* **155**,L181.
- Wright M. C. H., et al. 1990, *Astron. J.* 99,1299.